Journal of Nuclear Materials 510 (2018) 38–42

Contents lists available at ScienceDirect

Journal of Nuclear Materials

journal homepage: www.elsevier.com/locate/jnucmat

Thermodynamic properties of $Pb_3U_{11}O_{36}$

M. Cerini [a, b, *], O. Beneš [a], K. Popa [a], E. Macerata [b], J.-C. Griveau [a], E. Colineau [a], M. Mariani [b], R.J.M. Konings [a]

[a] European Commission, Joint Research Centre, Nuclear Safety and Security Directorate, P. O. Box 2340, 76125, Karlsruhe, Germany
[b] Politecnico di Milano, Department of Energy – Nuclear Engineering Division, Piazza Leonardo da Vinci 32, 20133, Milano, Italy

HIGHLIGHTS

- $Pb_3U_{11}O_{36}$ could be formed by chemical interaction between Pb and UO_2.
- Thermodynamic properties of $Pb_3U_{11}O_{36}$ are measured for the first time.
- Entropy at 298.15 K was derived by low temperature heat capacity measurements.
- High temperature heat capacity of $Pb_3U_{11}O_{36}$ was measured by drop calorimetry.
- Experimental thermodynamic data are in good agreement with the DFT-GGA values.

ARTICLE INFO

Article history:
Received 20 March 2018
Received in revised form
10 June 2018
Accepted 19 July 2018
Available online 20 July 2018

ABSTRACT

In order to progress in the development of Lead-cooled Fast Reactors, from the safety point of view it is essential to understand the chemical compatibility between liquid lead and uranium oxide. In the present work, entropy and heat capacity of $Pb_3U_{11}O_{36}$, a possible ternary compound coming from fuel-coolant chemical interaction, were determined for the first time. Entropy at 298.15 K was obtained from low temperature heat capacity measurements using the Physical Property Measurement System (PPMS) in the temperature range 2–300 K, while the high temperature heat capacity has been measured by a drop calorimeter from 373 K to 1200 K. The experimental thermodynamic properties were compared with the values computed by means of DFT-GGA simulations, obtaining a very good agreement.

1. Introduction

Some of the Fast Reactors concepts proposed by the Generation IV International Forum introduce liquid metals and molten salts as coolants [1–3]. The use of such peculiar coolants requires a good understanding of the chemical compatibility among the reactor's components. In the frame of the safety assessment of the Lead-cooled Fast Reactors (LFRs) the chemical compatibility between nuclear fuel and coolant has to be investigated to foresee the consequences of an accident leading to fuel-coolant interaction. In the proposed LFR systems the fuel is a mixed uranium-plutonium oxide (MOX) and the coolant is pure lead or lead-bismuth eutectic [4,5]. The multi-component and multi-phase nature of the fuel-coolant system is fated to become more complex as a consequence of a cladding failure event. The chemical composition of such system at equilibrium could be studied by thermodynamic analysis methods [6–8]. At a specified temperature and pressure, the most stable product will be the one with the lowest Gibbs free energy. The thermodynamic analysis requires the availability of a complete database with reliable thermodynamic data of all phases involved in the chemical system and is performed by a computer code based on the minimization of the free energy of the system. In our case, thermodynamic data on ternary compounds belonging to the U-O-Pb system are required to enable the study of the possible chemical interactions between the oxide fuels and the lead-based coolants. According to the ICSD database, only three possible intermediate compounds exist for this ternary system [9], which are $PbUO_4$ [10], Pb_3UO_6 [11] and $Pb_3U_{11}O_{36}$ [12]. For each of the above mentioned compounds, the crystallographic information and the lattice parameters are reported in literature, while thermodynamic properties are available only for $PbUO_4$ and Pb_3UO_6 [13].

In the present work, the heat capacity of $Pb_3U_{11}O_{36}$ has been determined for the first time by means of two experimental

* Corresponding author. European Commission, Joint Research Centre, Nuclear Safety and Security Directorate, P. O. Box 2340, 76125, Karlsruhe, Germany.
E-mail address: marta.cerini@polimi.it (M. Cerini).

https://doi.org/10.1016/j.jnucmat.2018.07.042
0022-3115/

techniques, the relaxation technique for low temperature heat capacity from 2 K to 300 K and the drop calorimetry for high temperature heat capacity determination for temperature range from 373 K to 1200 K. From the low temperature heat capacity measurements, the entropy value at 298.15 K was derived. In addition, the experimental values of entropy and heat capacity at 298.15 K were compared with the data computed using the Density Functional Theory (DFT) as implemented in the VASP (Vienna Ab-initio Simulation Package) code.

2. Experimental

2.1. Synthesis of compound $Pb_3U_{11}O_{36}$

The $Pb_3U_{11}O_{36}$ compound was prepared by solid state reaction, heating an appropriate mixture of commercial α-lead(II) oxide (Sigma-Aldrich, 99.98% trace metal basis) and $UO_{2.10}$ powders (COGEMA) at 1073 K for 24 h in an alumina crucible in air. The stoichiometry of $UO_{2.10}$ was confirmed by means of X-ray diffraction. During the synthesis, no-interactions were observed between the sample and the crucible. Several pellets of 3.5 mm diameter and 2–3 mm in height were produced by pressing and sintering the $Pb_3U_{11}O_{36}$ powders at 1073 K under air for 5 h.

2.2. X-ray diffraction analysis

Formation of the compound was confirmed by X-ray powder diffraction (XRD) using a Bruker D8 diffractometer mounted in a Bragg-Brentano configuration with a curved Ge (1, 1, 1) monochromator, a ceramic copper tube (40 kV, 40 mA) and equipped with a LynxEye position sensitive detector. The data were collected by step scanning in the angle range $10^\circ \leq 2\theta \leq 120^\circ$ at a 2θ step size of 0.0092° and XRD measurement was performed to determine the crystallographic purity of the compound. For the measurement, the powder was deposited on a silicon wafer to minimize the background and dispersed on the surface using isopropanol to avoid uranium powder dispersion in the device. The patterns were treated using the JANA 2006 software [14].

2.3. PPMS measurement

The low temperature heat capacity of a piece of $Pb_3U_{11}O_{36}$ of mass 28.107(5) mg was measured from 2 K to 300 K with a Physical Property Measurement System (PPMS-9T, Quantum Design) using the hybrid adiabatic relaxation method. First, the heat capacity contributions of the puck and grease layer (Apiezon N) were measured through the addenda protocol. Then the sample was fixed on the sapphire platform with grease, in order to guarantee a good thermal contact and to obtain the heat capacity of the sample [15]. Based on the comparison with standard materials, the estimated uncertainty of the measurements is better than 3% over the whole temperature range with a mass of the sample of few milligrams.

2.4. Drop calorimetry measurement

The enthalpy increment was measured on solid pieces of 43–48 mg using a Multi-Detector High Temperature Calorimeter (MDHTC-96, Setaram) with installed drop sensor. The aim of drop calorimetry is to evaluate the increment of enthalpy of the sample by its drop from ambient temperature to the detector, which is maintained at higher constant temperature. For more details about the technique, we refer to our earlier works [16]. The measurements were performed in a temperature range from 373 to 1200 K, using steps of 50 K, in air given the compound stability. Each isothermal measurement consisted of four drops of $Pb_3U_{11}O_{36}$ sample, surrounded by two drops of reference material (platinum ingots of 99.95 at.% purity). From the latter ones the sensitivity of the detector was obtained as a mean value and applied for determination of the enthalpy increment of the sample. Each drop has been separated by time intervals of 20 min, enough time to re-establish the monitored heat flow signal. A temperature calibration was performed using several high purity standard metals (Pb, Sn, Zn, Al, Ag and Ni) with different melting temperatures, in order to determine the temperature correction factor on the entire temperature range of the measurement, to be applied to the measured temperatures [17]. The heat flow signal analysis was performed using commercial available SetSoft 2000 software provided by SETARAM which is devoted for data processing.

3. Computational details

The DFT calculations were performed using the projector augmented wave (PAW) potentials [18,19] and the Perdew-Burke-Ernzerhof (PBE) spin-polarized Generalized Gradient Approximation (GGA) to compute the exchange-correlation energy [20] as implemented in VASP (Vienna Ab-initio Simulation Package) code [21,22]. The plane wave basis set and the number of k-points influence the convergence of the total energies. The plane wave cut-off energy was set to 500 keV because it depends on the largest cut-off energy in the pseudopotential file of each atomic species that constitutes the compound. For $Pb_3U_{11}O_{36}$ compound, the Brillouin zone of the unit cell crystal structure was sampled by a 4×4 x 4 Monkhorst – Pack k-point mesh [23,24]. The calculations were performed using finite Hubbard-U value U_{eff} of 0 eV. The U_{eff} value has been optimized during the validation process of the theoretical approach on the lattice parameters for Pb-containing binary oxides and intermetallics [25]. For all the other VASP parameters default values were adopted. The DFT-GGA simulations were performed on the unit cell of $Pb_3U_{11}O_{36}$ compound, which is characterized by two molecules per unit cell according to Pearson number oP100. The DFT-GGA calculations were performed to optimize the unit cell crystal structure of $Pb_3U_{11}O_{36}$ compound at minimum energy configuration using the stress tensor. Therefore, an additional DFT simulation was carried out for determining the vibrational frequencies of the investigated molecule, from which entropy and heat capacity were estimated using the crystal harmonic approximation. The calculation of vibrational frequencies was performed using the finite difference for the determination of the second derivative. The applied theoretical approach was validated on binary oxides, whose experimental data are available in literature, in order to determine the accuracy: a mean percentage accuracy of ±9.59% and ±4.46% for entropy and heat capacity at 298.15 K was obtained [25].

4. Results and discussion

4.1. XRD analyses

The synthesis resulted in phase-pure trilead undecauranate, $Pb_3U_{11}O_{36}$, as confirmed by room-temperature XRD analysis reported in Fig. 1. The structural analyses were performed by the Rietveld method using JANA2006 software [14]. The Rietveld refinement indicates that a single phase of orthorhombic $Pb_3U_{11}O_{36}$ (space group *Pmmn*, $a = 28.488(2)$ Å, $b = 8.388(1)$ Å, $c = 6.771(1)$ Å) was formed. The atomic positions were fixed based on the published structured obtained from neutron powder diffraction [11] and generate a calculated pattern in good agreement with experimental XRD data.

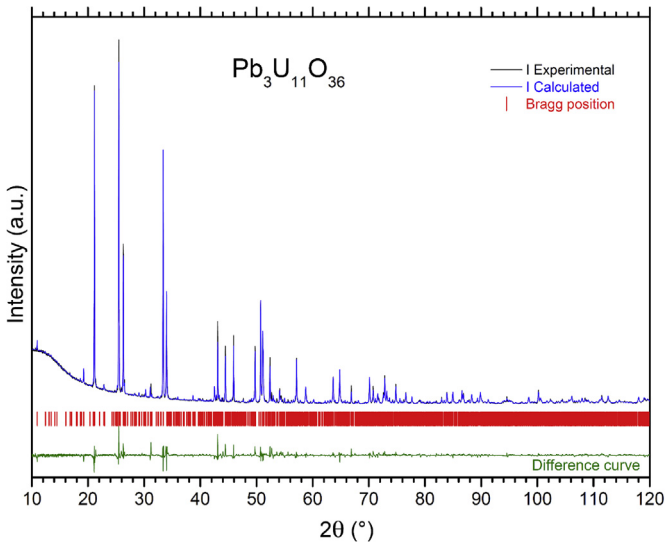

Fig. 1. Room-temperature Rietveld refinement of $Pb_3U_{11}O_{36}$ compound showing the (−) experimental, (−) calculated and (−) difference pattern. The vertical marks (|) indicate the positions of allowed Bragg reflections.

4.2. Heat capacity results

The low temperature heat capacity as a function of temperature is reported in Fig. 2 and Table S1. The results show a regular sigmoidal shape without anomalies in the investigated temperature range, in agreement with the trend observed for $PbUO_4$ and Pb_3UO_6 [13]. As shown in the inset in Fig. 2, the trend of $\frac{C_P}{T}$ versus T^2 is linear, thus indicating the absence of any magnetic anomaly below 10 K. At T = 0 K the extrapolation of $\frac{C_P}{T}$ does not yield zero and an electronic contribution $\gamma = 11\ mJ\ K^{-2}\ mol^{-1}$ can be determined. The results suggest that $Pb_3U_{11}O_{36}$ could present low temperature activated energy levels related to disorder or semi-conducting properties as already observed for other ternary compounds such as Pb_3UO_6 and $PbUO_4$ [13].

The low temperature heat capacity data were fitted according to the following equations [26].

- $C_P = B{\cdot}T + D{\cdot}T^3$ the Debye model from 0 K to 10 K;
- $C_P = A + B{\cdot}T + C{\cdot}T^2 + D{\cdot}T^3 + E{\cdot}T^{-1} + F{\cdot}T^{-2}$ from 10 K to 50 K;
- $C_P = A + B{\cdot}T + C{\cdot}T^2 + D{\cdot}T^3 + F{\cdot}T^{-2}$ from 50 K to 300 K.

The fit parameters are reported in Table S2. From the fitting, the heat capacity, entropy and enthalpy values at 298.15 K were derived: C_p (298.15 K) = 1006.4 J K^{-1} mol^{-1}, S (298.15 K) = 1276.0 J K^{-1} mol^{-1} and ($H^0_{298.15K}$ - H^0_{0K}) = 190087 J mol^{-1}. The derived room temperature C_p of $Pb_3U_{11}O_{36}$ is lower than the value of 1247.17 J K^{-1} mol^{-1} calculated by the Dulong-Petit law ($C_p \sim 3\,R{\cdot}n$, where n is the number of atoms in the compound and R is the universal gas constant) and this result is coherent with what was reported in literature for other uranates, such as $PbUO_4$, Pb_3UO_6 and Bi_2UO_6 [13,27]. For the $Pb_3U_{11}O_{36}$ compound the heat capacity follows the Dulong-Petit limit at a rather high temperature around 700 K, indicating that for this compound the associated Debye temperature is slightly enhanced [28] and it is estimated at 246 K [29].

At room temperature, the heat capacity of 1030.29 J K^{-1} mol^{-1} and the entropy of 1353.93 J K^{-1} mol^{-1} computed by DFT-GGA simulations are in good agreement with the experimental values reported in the present work. The computed values revealed a percentage error of +2.37% and +6.10% compared to the experimental heat capacity and entropy, respectively. The calculated thermodynamic properties at 298.15 K were evaluated with satisfactory accuracy because the percentage error falls within the accuracy range of the theoretical approach both for entropy and heat capacity. Moreover, these results are in line with the agreement obtained for other oxides considering thermodynamic parameters [25].

Above room temperature the enthalpy increments were measured by drop calorimetry and the obtained data are shown in the inset of Fig. 3 and listed in Table S3. The enthalpy increment data were fitted using a simultaneous linear regression taking into account selected low temperature heat capacity data and a constraint of C_p at room temperature determined earlier to ensure smooth transition between low and high temperature heat capacity functions. The resulting high temperature heat capacity of $Pb_3U_{11}O_{36}$ is shown in Fig. 3 with a confidence band highlighted by the dashed lines and is described by a Maier-Kelly type second order polynomial equation given below:

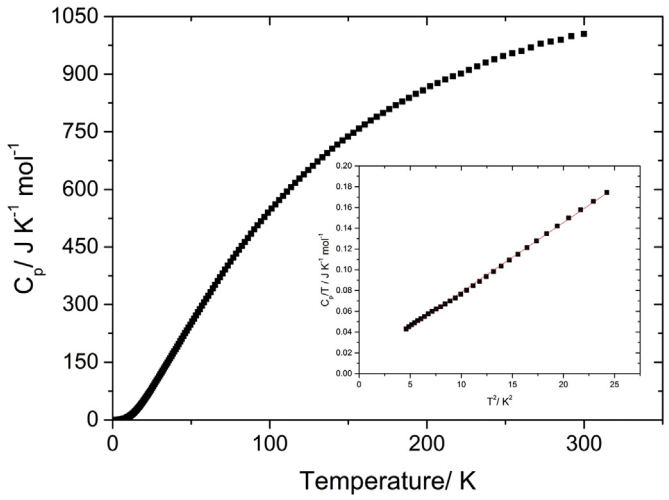

Fig. 2. Low temperature heat capacity of $Pb_3U_{11}O_{36}$ as a function of temperature. Inset: plot of C_p/T versus T^2 below 5 K.

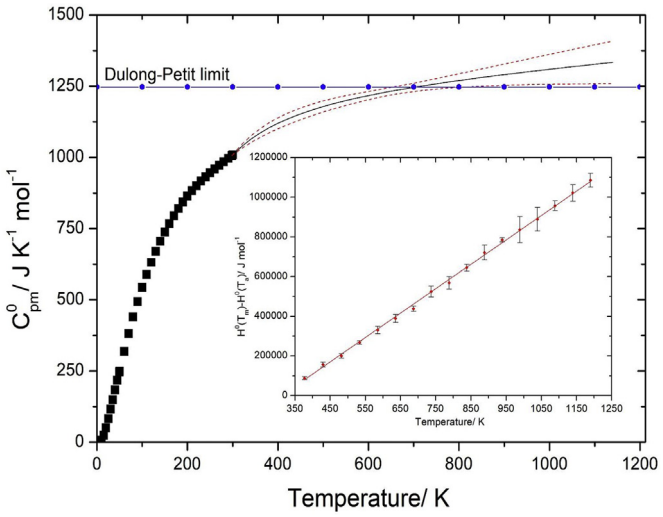

Fig. 3. The heat capacity of $Pb_3U_{11}O_{36}$ as function of temperature. (■) the low temperature heat capacity obtained by PPMS; (−) the heat capacity obtained by drop calorimetry; (- - -) the confidence band of the heat capacity. (- • -) the Dulong-Petit limit. Inset: plot of the measured entalphy increment ($H^0(T_m)$-$H^0(T_0)$) as function of temperature. (−) fit of the enthalpy increment data.

$$c_P\left[J\cdot K^{-1}mol^{-1}\right] = (1040.563\pm70.149) + (329.331\pm99.044)\cdot10^{-3}\cdot T - (11.764\pm3.722)\cdot10^{-6}\cdot T^{-2}$$

The high temperature heat capacity trend is similar to that observed for the other uranates and is given solely by lattice contribution, since no-magnetic fluctuations are visible and electronic contribution does not influence the high temperature heat capacity due to the very low γ value [13,27,30]. The C_p trend is remaining very close to the Dulong-Petit value (150 R) up to T = 1200 K.

The heat capacity and entropy computed by DFT-GGA approach were compared with the experimental data on the entire temperature range of this study as shown in Figs. 4 and 5, respectively. It is evident from Fig. 4 that the experimental high temperature heat capacity is higher than the theoretical data. The reason of this discrepancy could be attributed to the additional contributions could arising from the electron phonon coupling which are not taken into account in the theoretical calculation. Moreover, the difference between the experimental and computed entropy in Fig. 5 be related to the percentage error determined at 298.15 K as previously explained.

5. Conclusions

The thermodynamic properties of the compound $Pb_3U_{11}O_{36}$ were experimentally determined for the first time. Measurements at low temperature enabled to evaluate heat capacity, entropy and enthalpy at 298.15 K. Combining the low temperature data with the high temperature heat capacity values obtained by drop calorimetry, the heat capacity of $Pb_3U_{11}O_{36}$ in the temperature range from 2 K to 1200 K was obtained. The experimental values for entropy and heat capacity at 298.15 K were compared with the data computed by DFT-GGA simulations and statistical thermodynamics equations, obtaining a very satisfactory agreement with percentage error deviations of +2.37% and +6.10% for heat capacity and entropy, respectively. Within the development of Lead-cooled Fast Reactors, further studies on the possible interaction products are fundamental in order to fully understand the behavior of nuclear fuel in interaction with liquid lead. In addition, it was demonstrated that computational DFT simulations could be strong tools to obtain valuable data of the Pb − U − O compounds.

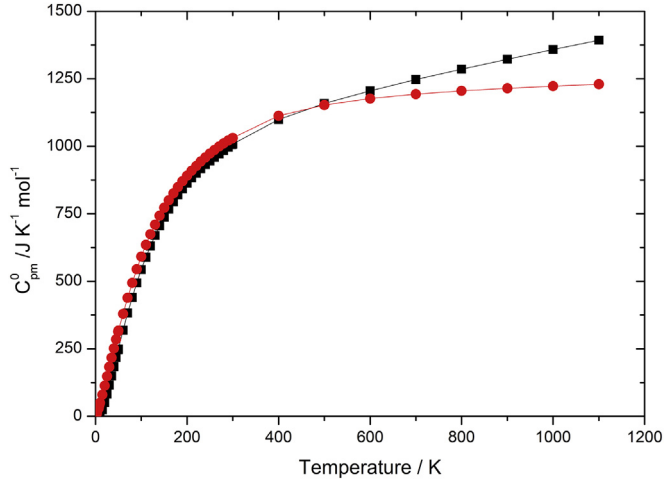

Fig. 4. The heat capacity of $Pb_3U_{11}O_{36}$ as function of temperature. (■) the experimental heat capacity obtained from PPMS and drop calorimeter; (•) the calculated heat capacity derived by DFT-GGA simulation.

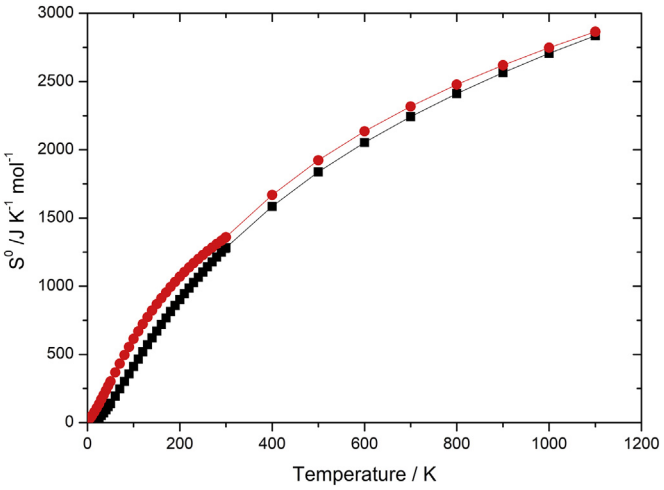

Fig. 5. The entropy of $Pb_3U_{11}O_{36}$ as function of temperature. (■) the experimental entropy derived from PPMS and drop calorimeter; (•) the calculated entropy derived by DFT-GGA simulation.

Acknowledgements

This work was developed within the "**Safe exploitation related chemistry for HLM reactors** (SEARCH)" Collaborative Project (Contract Number: 295736) in the Seventh Framework Programme of the European Commission. The authors acknowledge Daniel Bouëxière and Michael Holzhäuser for the technical support and Jean-François Vigier for fruitful discussions. The theoretical part of the present work was performed using the ab-initio total-energy and molecular-dynamics program VASP (Vienna ab-initio simulation package) developed at the Fakultat fur Physik of the Universitat Wien. The calculations were carried out thanks to the computing resources awarded by a public tender within the LISA Initiative promoted by Regione Lombardia and CINECA consortium.

Appendix A. Supplementary data

Supplementary data related to this article can be found at https://doi.org/10.1016/j.jnucmat.2018.07.042.

References

[1] Annual Report, Generation IV International forum, 2014.
[2] P. Wydler, Liquid metal cooled reactors, Chimia 59 (2005) 970–976.
[3] IAEA NUCLEAR ENERGY SERIES No, NP-T-1.6, Liquid Metal Coolants for Fast Reactors Cooled by Sodium, Lead, and Lead-Bismuth Eutectic, 2012.
[4] J.-F. Vigier, P.M. Martin, L. Martel, D. Prieur, A.C. Scheinost, J. Somers, Structural investigation of $(U_{0.7}Pu_{0.3})O_{2-x}$ mixed oxide, Inorg. Chem. 54 (2015) 5358–5365.
[5] J.-F. Vigier, K. Popa, V. Tyrpekl, S. Gardeur, D. Freis, J. Somers, Interaction study between MOX fuel and eutectic lead-bismuth coolant, J. Nucl. Mater. 467 (2015) 840–847.
[6] S. Imoto, Chemical state of fission products in irradiated UO_2, J. Nucl. Mater. 140 (1986) 19–27.
[7] E.H.P. Cordfunke, R.J.M. Konings, Chemical interactions in water-cooled nuclear fuel: a thermochemical approach, J. Nucl. Mater. 152 (1988) 301–309.
[8] Z.S. Li, X.J. Liu, C.P. Wang, Thermodynamic modelling of the Pb-U and Pb-Pu systems, J. Nucl. Mater. 403(210) 1–6.
[9] M. Hellenbrandt, The inorganic crystal structure database (ICSD) – present and future, Crystallography Reviews 10 (2004) 17–22.
[10] T.L. Cremers, P.G. Eller, E.M. Larson, Single-crystal structure of lead uranate (VI), Acta Crystallogr. C 42 (1986) 1684–1685.
[11] M. Sterns, The crystal structure of Pb_3UO_6, Acta Crystallogr. 23 (1967) 264.
[12] D. Ijdo, $Pb_3U_{11}O_{36}$, a Rietveld refinement of neutron powder diffraction data, Acta Crystallogr. C 49 (1993) 654–656.

[13] K. Popa, O. Beneš, D. Staicu, J.-C. Griveau, E. Colineau, P. Raison, J.-F. Vigier, G. Pagliosa, M. Sierig, O. Valu, J. Somers, R.J.M. Konings, Thermal properties of $PbUO_4$ and Pb_3UO_6, J. Nucl. Mater. 479 (2016) 189–194.
[14] V. Petricek, M. Dusek, L. Palatinus, Crystallographic computing system JANA2006: general features, Kristallogr. - Cryst. Mater. 229 (2014).
[15] J. Lashley, M. Hundley, A. Migliori, J. Sarrao, P. Pagliuso, T. Darling, M. Jaime, J. Cooley, W. Hults, L. Morales, D. Thoma, J. Smith, J. Boerio-Goates, B. Woodfield, G. Stewart, R. Fisher, N. Phillips, Critical examination of heat capacity measurements made on a Quantum Design physical property measurement system, Cryogenics 43 (2003) 369–378.
[16] O. Beneš, P. Gotcu-Freis, F. Schworer, R.J.M. Konings, Th. Fanghanel, the high temperature heat capacity of NpO_2, J. Chem. Thermodyn. 43 (2011) 651–655.
[17] O. Beneš, R.J.M. Konings, D. Sedmidubsky, M. Beilmann, O.S. Valu, E. Capelli, M. Salanne, S. Nichenko, A comprehensive study of the heat capacity of CsF from T = 5 K to T = 1400 K, J. Chem. Thermodyn. 57 (2013) 92–100.
[18] G. Kresse, J. Furthmuller, Efficient interactive schemes for ab-initio total energy calculations using a plane wave basis set, Phys. Rev. B 54 (1996) 11169.
[19] G. Kresse, D. Joubert, Phys. Rev. B 59 (1999) 1758.
[20] J. Perdew, K. Burke, M. Ernzerhof, Generalized gradient approximation made simple, Phys. Rev. Lett. 77 (1996) 3865–3868.
[21] J. Hafner, Ab-initio simulations of materials using VASP: density-functional theory and beyond, J. Comput. Chem. 29 (2008) 2044–2078.
[22] G. Kresse, J. Hafner, Ab-initio molecular dynamics for liquid metals, Phys. Rev. B 47 (1993) 558–561.
[23] P. Blochl, O. Jepsen, O. Andersen, Improved tetrahedron method for Brillouin-zone integrations, Phys. Rev. B 49 (1994) 16223–16233.
[24] H. Monkhorst, J. Pack, Special points for Brillouin-zone integrations, Phys. Rev. B 13 (1976) 5188–5192.
[25] M. Cerini, E. Macerata, M. Giola, M. Mariani, C. Cavallotti, DFT-gga Predictions of Thermodynamic Parameters in Solid Phase for Binary Compounds of Actinides and Fission Products Proceedings of Global 2015, Paris, France, September 20-24, 2015, SFEN, ISBN 978-1-4951-6286-2 5451, 2015, pp. 1361–1366.
[26] D. Thomas, M. Abdel-Hafiez, T. Gruber, R. Huttl, J. Seidel, A.U.B. Wolter, B. Buchner, J. Kortus, F. Mertens, The heat capacity and entropy of lithium silicades over the temperature range from 2 to 873 K, J. Chem. Thermodyn. 64 (2013) 205–225.
[27] K. Popa, O. Beneš, P.E. Raison, J.-C. Griveau, P. Poml, E. Colineau, R.J.M. Konings, J. Somers, Heat capacity of Bi_2UO_6, J. Nucl. Mater. 465 (2015) 653–656.
[28] A.L. Smith, J.-C. Griveau, E. Colineau, P.E. Raison, R.J.M. Konings, Low temperature heat capacity of α-Na_2NpO_4, Thermochimica Acta 617 (2015) 129–135.
[29] B.E. Lang, Specific Heat and Thermodynamic Properties of Metallic System: Instrumentation and Analysis, Brigham Young University, 2006, p. 785.
[30] K. Popa, E. Colineau, F. Wastin, R.J.M. Konings, The heat capacity of $BaUO_4$, J. Chem. Thermodyn. 39 (2007) 104–107.